Printed in the Republic of Korea
ANALYTICAL SCIENCE & TECHNOLOGY
Vol. 38 No. 2, 129-145, 2025
https://doi.org/10.5806/AST.2025.38.2.129

Development of a volumetric image gas sensor for measuring gas emission concentrations and diffusivity in polymer materials charged with various gases

Ji Hun Lee★ and Sang Koo Jeon

Hydrogen Energy Group, Korea Research Institute of Standards and Science, Daejeon 34113, South Korea

(Received February 1, 2025; Revised March 10, 2025; Accepted March 17, 2025)

Abstract: Gas sensors play an important role in various areas, including industrial safety, environmental monitoring, gas infrastructure and medical diagnostics. These sensors identify and measure the concentration of specific gases in various environments, ensuring operational safety and efficiency by providing accurate on-site measurement. Gas sensors are engineered for high sensitivity, stability, and reliability, while also being required to be cost-effective, responsive, and compact. To respond these needs, the volumetric image gas sensor based on volumetric measurement is developed. The sensor works by quantifying the volume of gas based on the emitted gas. This sensor is capable of determining gas uptake, solubility and diffusivity in gas-charged polymers under high pressure. The sensor delivers quick responses within a second and can detect gas concentrations from 0.01 wt·ppm to 1400 wt·ppm, with changeable sensitivity and measurement ranges. Performance testing verifies the reliability of the sensor, its ability to adapt to different measurement ranges and its stability under temperature and pressure variations. As a result, this sensor system enables real-time detection and analysis of gas transport properties in pure gases like H_2, He, N_2, O_2, and Ar, making it ideal for pure gas sensing applications.

Key words: gas sensor, volumetric analysis, gas uptake, diffusivity, polymer

1. Introduction

Gas sensing is essential for safety, especially in environments with hazardous gases like hydrogen or carbon monoxide.[1-10] Early detection of gas emissions and leaks can prevent accidents, fires and other risks. It is vital for environmental monitoring, the detection of pollutants and the preservation of air quality. An accurate gas sensor is key to optimize operations, especially for renewable energy sources such as hydrogen. By ensuring precise measurement of H_2 gas emission, it improves safety, efficiency, and performance across the hydrogen production, storage and distribution stages.[11-22]

Polymer materials play a crucial role in hydrogen infrastructure.[23-45] Polymer materials like O-ring seal, gasket, liner and non-metallic pipeline are widely used. It is built to endure hydrogen-rich environments.

★ Corresponding author
Phone : +82-(0)42-868-5759
E-mail : ljh93@kriss.re.kr

However, these polymers are subjected to harsh conditions including wide temperature fluctuations and pressure variations. These conditions can cause seal damage, poor contact with gloves and gas permeation through polymer seals, potentially leading to hydrogen leakage.[46-52]

Gas permeation including hydrogen in polymers also occurs when gases pass through the polymer matrix due to diffusion. This process is influenced by factors such as temperature, pressure and the chemical nature of both gas and polymer.[53-55] In addition, the permeation rate can vary based on the polymer's structure, composition, filler content and the type of gas involved, with amorphous polymers typically having higher permeability compared to crystalline ones. Gas permeation is an important consideration in applications like gas storage and delivery, where polymers need to have low gas diffusion/permeability to avoid leakage and maintain system integrity.

Gas sensors are crucial for precisely detecting gas concentrations and leaks in applications like fuel cells, storage facilities, and transportation systems.[56,57] Various gas sensors are employed based on different sensing principles with its own characteristic. Infrared (IR) gas sensing[58-66] works on the principle that gas molecules absorb infrared light of specific wavelengths. The intensity of the absorbed light is measured and correlated to the concentration of the target gas. IR gas sensing offers key benefits such as high sensitivity, selectivity, and ability to detect gases across a broad concentration range. For example, it is widely used in industrial safety systems to monitor gas leaks in chemical plants. However, its performance can be influenced by environmental factors like temperature and humidity, necessitating regular calibration to maintain accuracy.

Semiconductor gas sensors[67-78] operate based on the principle that gas molecules interact with the surface of a semiconductor (typically metal oxides), causing a change in its electrical resistance. The change in resistance is measured and intercorrelated to concentration of the target gas. These sensors have advantages like low cost, fast response, and compact size, making them ideal for applications like air quality monitoring in urban environments. However, they can be affected by factors like temperature, pressure, and humidity. For instance, in industrial settings, these sensors may show cross-sensitivity to gases like methane, which can impact their accuracy in detecting specific pollutants.

Catalytic combustion gas sensors[79-85] work by detecting gases through the catalytic oxidation of the target gas on a heated catalyst surface, which generates heat. This heat change is measured and used to determine the gas concentration. These sensors offer high sensitivity to combustible gases and reliable detection of flammable gases at low concentrations. However, their lifespan is limited, particularly when exposed to poisons such as silicone or lead, and they may need frequent maintenance to maintain accuracy.

An optical spectroscopy gas sensor[86-99] works by the principle that gas molecules absorb or emit light at specific wavelengths. When light passes through a gas sample or is reflected from it, the gas molecules absorb light at characteristic absorption bands corresponding to their molecular structure. The amount of absorbed light is then measured, which is related to the gas concentration. Optical spectroscopy gas sensors offer high sensitivity, non-destructive measurement, and accurate detection of low gas concentrations. They can identify a broad spectrum of gases and are generally unaffected by interference from other substances. However, they can be influenced by environmental factors like temperature, pressure, and the presence of other gases in complex mixtures. These sensors are commonly used in air quality monitoring and environmental research, where precise gas detection is essential.

An electrochemical gas sensor[100-118] detects gases through a chemical reaction between the target gas and electrodes in an electrolyte, generating an electrical current proportional to the gas concentration. These sensors have high sensitivity, low power consumption and excellent selectivity for specific gases. However, they can be affected by temperature and humidity and their lifespan may be shortened due to electrode or electrolyte degradation. Electrochemical sensors are commonly used in personal gas detectors for

safety in industrial environments, where quick, accurate gas detection is critical.

Finally, gas chromatography[119-134] and mass spectrometry[135-147] provide highly precise analysis and commonly are used in research and laboratory settings. Gas chromatography separates from gas mixtures and analyzes individual components, while mass spectrometry identifies gas molecules based on their mass after ionization. However, these sensing systems are expensive and require regular maintenance, making them unsuitable for real-time field monitoring.

The conventional gas sensing technologies face challenges in specimen size, sensitivity, selectivity and environmental stability. These limitations highlight the need for advanced gas sensors that are compact, have rapid response times, high sensitivity and robust performance to ensure safety in real-time gas monitoring.

Thus, the volumetric gas sensors with the performance to meet these requirements is proposed based on the image processing algorithm and digital camera and graduated cylinder.[5,148] This sensing system aims to provide the real-time monitoring by connecting to a computer via a GPIB interface and using a diffusion analysis program[149-151] to accurately calculate gas concentration/diffusion in the polymer specimen with the insensitivity to temperature/pressure changes. This detection system can easily measure gas concentration and diffusion in the polymer specimen in real-time on-site without any chemical interactions with gas.

The developed gas sensor system has demonstrated versatility in detecting and analyzing gases such as H_2, He, O_2, N_2, and Ar, while monitoring gas adsorption and diffusion in polymers in real-time. It offers consistent performance in sensitivity, stability and response time. The sensor technology presented provides a compact, portable solution that can replace bulky equipment. It has potential applications not only in hydrogen infrastructure safety management but also in the gas industry for real-time gas detection. We represented the principles, procedures, results and characteristics of this sensing method. Thus, the developed gas sensing method provides valuable insights into the diffusion properties, leakage and sealing capabilities of O-rings under high-pressure conditions.

2. Experimental

2.1. Sample preparation and high-pressure gas charging

The developed gas sensor measures gas concentration and diffusion coefficient during the desorption process of gases exposed to high pressure from polymer specimens. The polymers tested include low-density polyethylene (LDPE), commonly used for containers, plastic bags and gas transport pipes due to its gas-barrier properties. Ethylene propylene diene monomer (EPDM) is used in O-ring seal materials for high-pressure gas storage vessel. This gas detection system enables the determination of permeation properties (solubility, diffusivity and permeability) of the polymer samples.

The LDPE specimen was produced by King Plastic Corporation, utilizing advanced antimicrobial technology. Details on the composition and density of the polymer samples are available in prior studies.[3,151] The EPDM was degassed by heat treatment at 60 °C for 48 hours. The polymer samples were prepared in the following cylindrical shapes and dimensions:

– LDPE : radius (R) 9.51 mm, thickness (T) 4.89 mm, 1.57 mm

– EPDM : radius (R) 9.51 mm, thickness (T) 2.56 mm

For high-pressure gas exposure, a SUS 316 chamber with specific volume was used at room temperature and specified pressure conditions. The gas exposure was performed in the pressure ranging from 2 MPa to 10 MPa. The purity of the gases used was as:

• H_2: 99.999 %, He: 99.999 %, N_2: 99.999 %, O_2: 99.99 %, Ar: 99.999 %

Before gas exposure, the chamber was purged three times with the corresponding gas from 0.5 MPa to 1 MPa. Samples were then exposed to the gas at the specified pressure for 24-48 hours, with H_2 and He exposed for 24 hours due to their fast diffusion rates, while N_2, O_2, and Ar were exposed for 48 hours due to their slower diffusion rates. A maximum gas

exposure of 48 hours was sufficient to reach the equilibrium for gas sorption into specimen. Additionally, since thicker specimens require a longer exposure time, LDPE specimens of 4.89 mm thickness were used for H_2 and He, while 1.57 mm thick specimens were used for N_2, O_2, and Ar to minimize the difference in gas exposure time.

2.2. Volumetric measurement of the released gas from charged polymers

A volumetric measurement (VM) technique was developed to assess gas diffusion and permeation. This method involves measuring the gas concentration released from a specimen after high-pressure gas charging and decompression. *Fig.* 1 shows the volumetric image sensor system used to quantify the released gas at room temperature. The system includes a high-pressure chamber (*Fig.* 1(a)) for gas exposure and a cylinder (*Fig.* 1(b)) immersed in a water container.

After high-pressure gas charging and decompression, the specimen was placed in the upper air space of a cylinder, as shown in *Fig.* 1(b). The gas released from the specimen caused the water level in the cylinder to gradually decrease. As a result, the pressure (P) and volume (V) of the gas inside the cylinder changed over time. The water level in cylinder has crescent shape, as shown in *Fig.* 1(b).

The gas in the cylinder follows the ideal gas law, PV = nRT, where R is the gas constant (8.20544×10^{-5} m³·atm/(mol·K)), T is the temperature inside the cylinder and n is the number of moles of gas released. The changes in pressure $P(t)$ and volume $V(t)$ of the gas in the cylinder can be described as follows:[152]

$$P(t) = P_o(t) - \rho g h(t),\ V(t) = V_o - V_s - V_h(t) \qquad (1)$$

where P_o is the external pressure outside the cylinder, g is the gravitation acceleration and ρ is the density of distilled water. The $h(t)$ indicates water level within the graduated cylinder over time, while V_o is the combined volume of gas and water inside the cylinder, measured relative to the water level in the container. $V_h(t)$ is the time-dependent volume of water in the cylinder, and V_s indicates the volume occupied by the sample.

The amount of gas released by the polymer specimen was quantified by tracking the water level position [$V_h(t)$] over time. The total moles of gas released [$n(t)$)] were then calculated by measuring the total gas volume [$V(t)$] in the cylinder, which corresponds to the decrease in the water level, as expressed by the

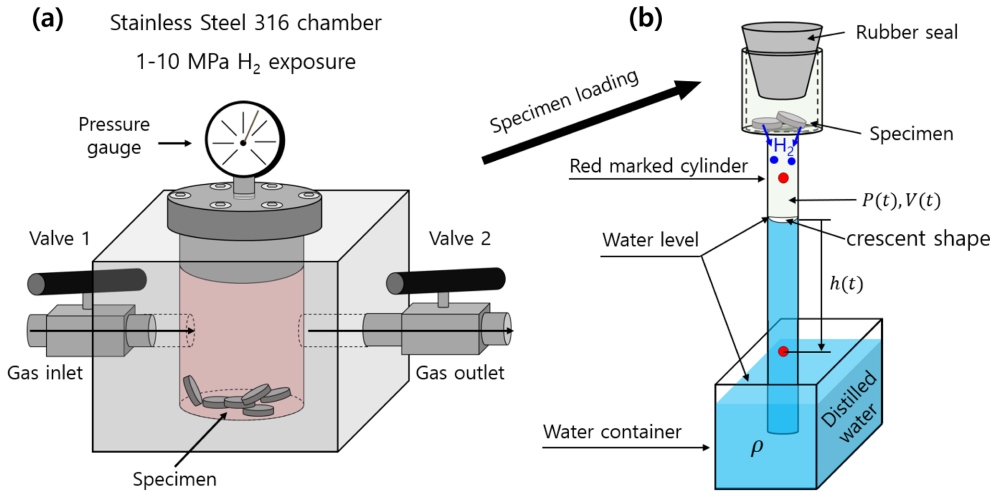

Fig. 1. Volumetric image sensor system to measure the gas uptake and diffusivity emitted by a specimen after exposure to HP gas and decompression. (a) Specimen exposed to gas in a high-pressure chamber. (b) After decompression in the chamber, the specimen was loaded into a graduated cylinder. The cylinder was immersed in a water container and gas emission measurements were conducted. Blue in cylinder indicates water. The ● in the graduated cylinder represents the gas emitted from the exposed sample.

following:[152]

$$n(t)=\frac{P(t)V(t)}{RT(t)}=\frac{P(t)[V_A+V_H(t)]}{RT(t)}=\frac{P_0[1+\beta(t)][V_A+V_h(T)]}{RT_0[1+\alpha(t)]}$$

$$\cong\frac{P_0}{RT_0}[V_A+V_H(t)+V(t)(\beta(t)-\alpha(t))]=n_A(t)+n_H(t) \quad (2)$$

with

$$n_A(t)=\frac{P_0}{RT_0}V_A,\ n_H(t)=\frac{P_0}{RT_0}[V_H(t)+V(t)(\beta(t)-\alpha(t))]$$

$$\alpha(t)=\frac{T(t)-T_0}{T_0},\ \beta(t)=\frac{P(t)-P_0}{P_0},$$

In Eq. (2), T_0 and P_0 are the initial temperature and pressure of the gas in the graduated cylinder, respectively. $V(t)$ is the total volume, consisting of the remaining initial air volume (V_A) and the released gas volume [$V_H(t)$], so that $V(t)=V_A+V_H(t)$ .n_A denotes the initial mole number of air and $n_H(t)$ refers to the time-dependent mole number of gas corresponding to the increase in gas volume due to its release. Therefore, $n_H(t)$ was converted to the gas concentration, [$C(t)$ emitted per unit mass from the specimen as :

$$C(t)\ [\text{wt·ppm}]=n_H(t)\ [\text{mol}]\times\frac{m_{Gas}\left[\frac{g}{\text{mol}}\right]}{m_{sample}[\text{g}]}\times10^6 \quad (3)$$

For example, the molar mass of H_2 gas, m_{H2} [g/mol] is 2.016 g/mol. The molar mass of nitrogen gas m_{N2} [g/mol] is 28.013 g/mol. m_{sample} is the specimen mass. In Eqs. (2) and (3), the time-dependent mole number of gas, $n_H(t)$, was converted to the gas mass concentration, [$C(t)$], by the factor, $k=\left[\frac{m_{Gas}}{m_{sample}}\right]$. $n_H(t)$ and $C(t)$ are affected by the fluctuations of temperature and pressure in the laboratory environments. To ensure precise measurements, it's essential to compensate for these variations. This compensation can be achieved through automated programs according to Eq. (3). That is., the terms, $V(t)(\beta(t)-\alpha(t))$, is the volume change in the $V_H(t)$, caused by the temperature and pressure change. The compensation indicates the application of $V(t)(\beta(t)-\alpha(t))$ calculation in Eq. (3). Thus, the insensitivity of the sensor to variations in temperature/pressure indicates application of automatic compensation by program.

The release of gas was tracked by monitoring changes in water level measurement using image processing algorithm via digital camera in front of the graduated cylinder. The procedure for obtaining the water level (emitted gas volume) from water level measurement is described in previous works.[5,148]

2.3. Diffusion analysis program for obtaining transport parameters

Gas emission from the gas-exposed sample follows Fickian diffusion, thus, the concentration of the emitted gas, $C_E(t)$, is calculated as :[153,154]

$$C_E(t)/C_\infty=1-\frac{32}{\pi}\times\left[\sum_{n=0}^{\infty}\frac{\exp\left\{\frac{-(2n+1)^2\pi^2Dt}{l^2}\right\}}{(2n+1)^2}\right]\times$$

$$\left[\sum_{n=1}^{\infty}\frac{\exp\left\{-\frac{D\beta_n^2t}{\rho^2}\right\}}{\beta_n^2}\right]=1$$

$$-\frac{32}{\pi^2}\times\left[\frac{\exp\left(-\frac{\pi^2Dt}{l^2}\right)}{1^2}+\frac{\exp\left(-\frac{3^2\pi^2Dt}{l^2}\right)}{3^2}+\ldots,\frac{\exp\left(-\frac{(2n+1)^2\pi^2Dt}{l^2}\right)}{(2n+1)^2}+\ldots\right]$$

$$\times\left[\frac{\exp\left(-\frac{D\beta_1^2t}{\rho^2}\right)}{\beta_1^2}+\frac{\exp\left(-\frac{D\beta_2^2t}{\rho^2}\right)}{\beta_2^2}+\ldots+\frac{\exp\left(-\frac{D\beta_n^2t}{\rho^2}\right)}{\beta_n^2}+\ldots\right] \quad (4)$$

where β_n represents root of zeroth-order Bessel function, $J_0(\beta_n)$. This equation corresponds to solution of Fick's second diffusion equation for a cylindrical shaped specimen. $c_e(t=0)=0$ and $c_e(t=\infty)=c_\infty$ is saturated gas concentration at infinite time, indicating total gas uptake (emission content). D is the gas diffusivity. l and ρ are thickness and radius of cylindrical sample, respectively.

To accurately calculate using Eq. (4), many terms in the product of two summations are involved. Therefore, a dedicated diffusion analysis program was developed to precisely calculates C_∞ and D. This program uses a nonlinear optimization algorithm[142,155] to accurately compute $C_E(t)$ and D from the experi-

mental data by solving the complicated Eq. (4).

3. Results and Discussion

3.1. Volumetric measurement

After decompressing a specimen enriched with nitrogen under high pressure, the released gas concentration and diffusivity were determined using the VM method with a graduated cylinder (*Fig.* 1). The water level in VM method is measured by employing image processing algorithm and a digital camera.[148] *Fig.* 2 displays the measured and fitted results for

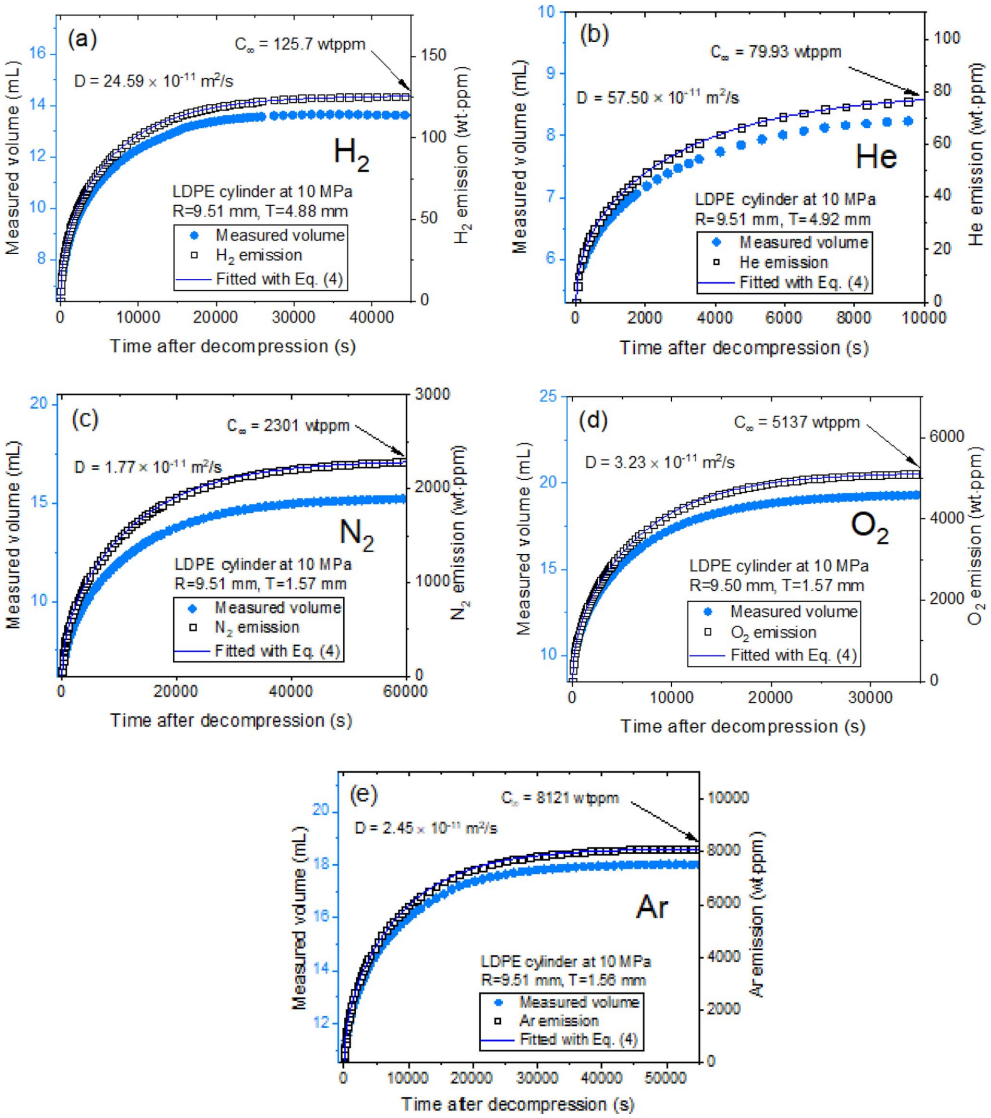

Fig. 2. Gas uptake and diffusivity determined from five gases in a cylindrical LDPE specimen by volumetric measurement using image processing algorithm and a digital camera. (a) through (e) : Measured corresponding gas volume (blue filled circle) transformed from the measured water level and emitted gas emission (black open square) transferred from measured gas volume in unit of wt·ppm. The blue line represents the fitted result using Eq. (4). Diffusion parameters, D and C_∞, calculated using a diffusion program based on Eq. (4). The blue line represents the fitted data using Eq. (4), with gas diffusivity the total gas uptake marked by a blue arrow. Here, R is the radius of the cylindrical specimen. T is the thickness of the cylindrical specimen.

five gases (H_2, He, N_2, O_2 and Ar) in the cylindrical LDPE specimen determined from the water level measurement by VM. The left sides of *Fig.* 2(a) through (e) show corresponding emitted gas volume (blue filled circle) transferred from water level measurement. The right sides of *Fig.* 2(a) through (e) represent corresponding gas emission data (black open square). The diffusion parameters, D and C_∞, are derived by a diffusion program by Eq. (4). The blue line in *Fig.* 2 represents the fitted result using

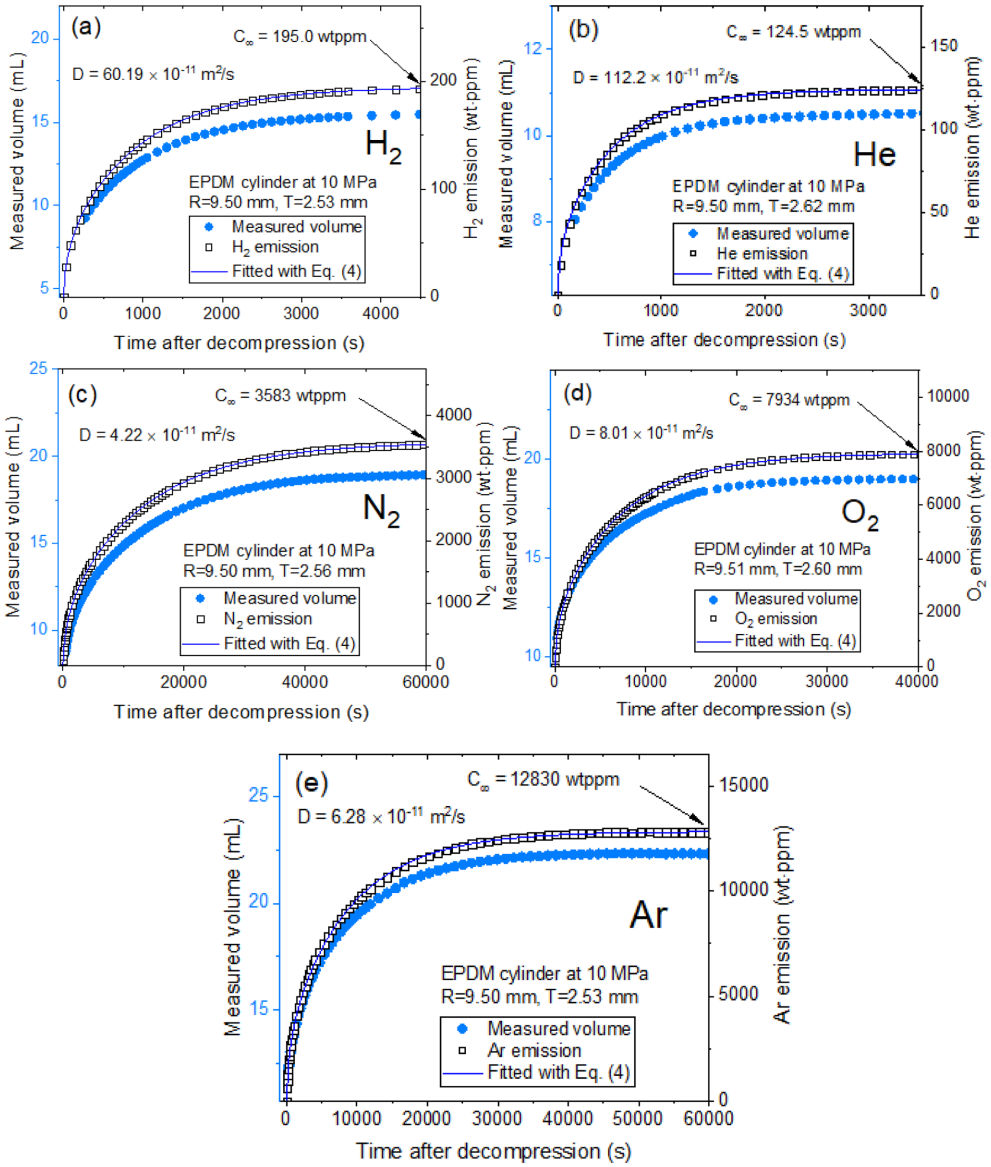

Fig. 3. Gas uptake and diffusivity determined from five gases in a cylindrical EPDM specimen by volumetric measurement using image processing algorithm and a digital camera. (a) through (e) : Measured corresponding gas volume (blue filled circle) transformed from the measured water level and emitted gas emission (black open square) transferred from measured gas volume in unit of wt·ppm. The blue line represents the fitted result using Eq. (4). Diffusion parameters, D and C_∞, calculated using a diffusion program based on Eq. (4). The blue line represents the fitted data using Eq. (4), with gas diffusivity the total gas uptake marked by a blue arrow. Here, R is the radius of the cylindrical specimen. T is the thickness of the cylindrical specimen.

Eq. (4), with diffusivity and the total gas uptake marked by a blue arrow. As shown in *Fig.* 2(a) through (e), single-mode gas emission behaviors for all gases in LDPE were observed under time-varying gas emission measurement. The single-mode gas emission in LDPE results from gas diffusion into the amorphous phase.

In similarity with *Figs*. 2 and 3(a) through (e) display the measured and fitted results for five gases in the cylindrical EPDM specimen determined from VM measurement. The left and right sides of *Fig*. 3(a) through (e) show corresponding gas volume (blue

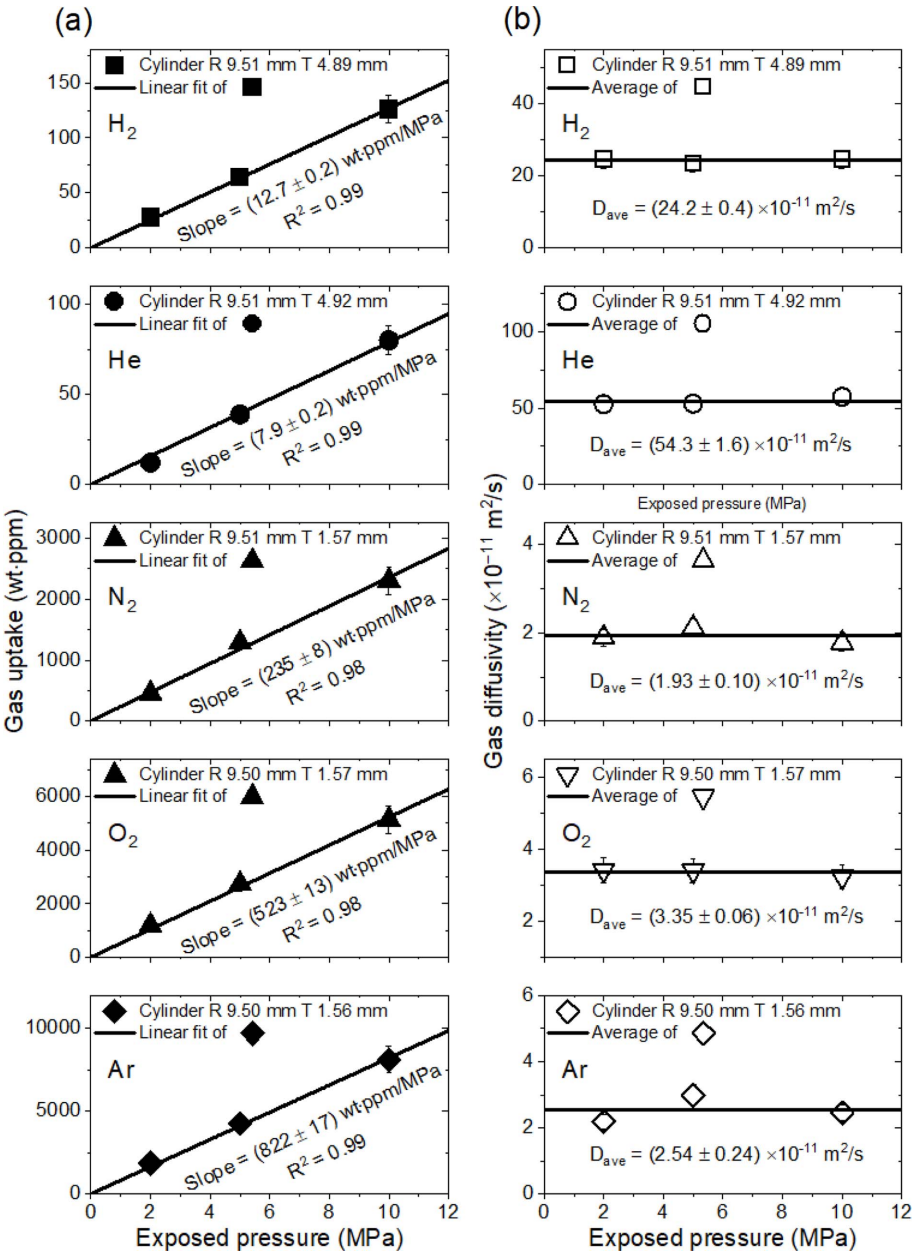

Fig. 4. (a) Gas uptake, (b) diffusivity versus exposed pressure for the five gases in cylindrical LDPE. R and T represent the radius and thickness of cylindrical LDPE, respectively.

filled circle) and gas emission content (black open square), respectively. The right sides of *Fig.* 3(a) through (e) represent the diffusion parameters, D and C_∞, derived using a diffusion program by Eq. (4). The blue line in *Fig.* 3 represents the fitted data using Eq. (4), with diffusivity and the total gas uptake marked by a blue arrow. As shown in *Fig.* 3(a) through (e), single-mode gas emission behaviors for all gases in EPDM were observed under time-varying gas emission measurement.

Fig. 4 show the corresponding gas uptake and diffusivity of LDPE as a function of exposed pressure

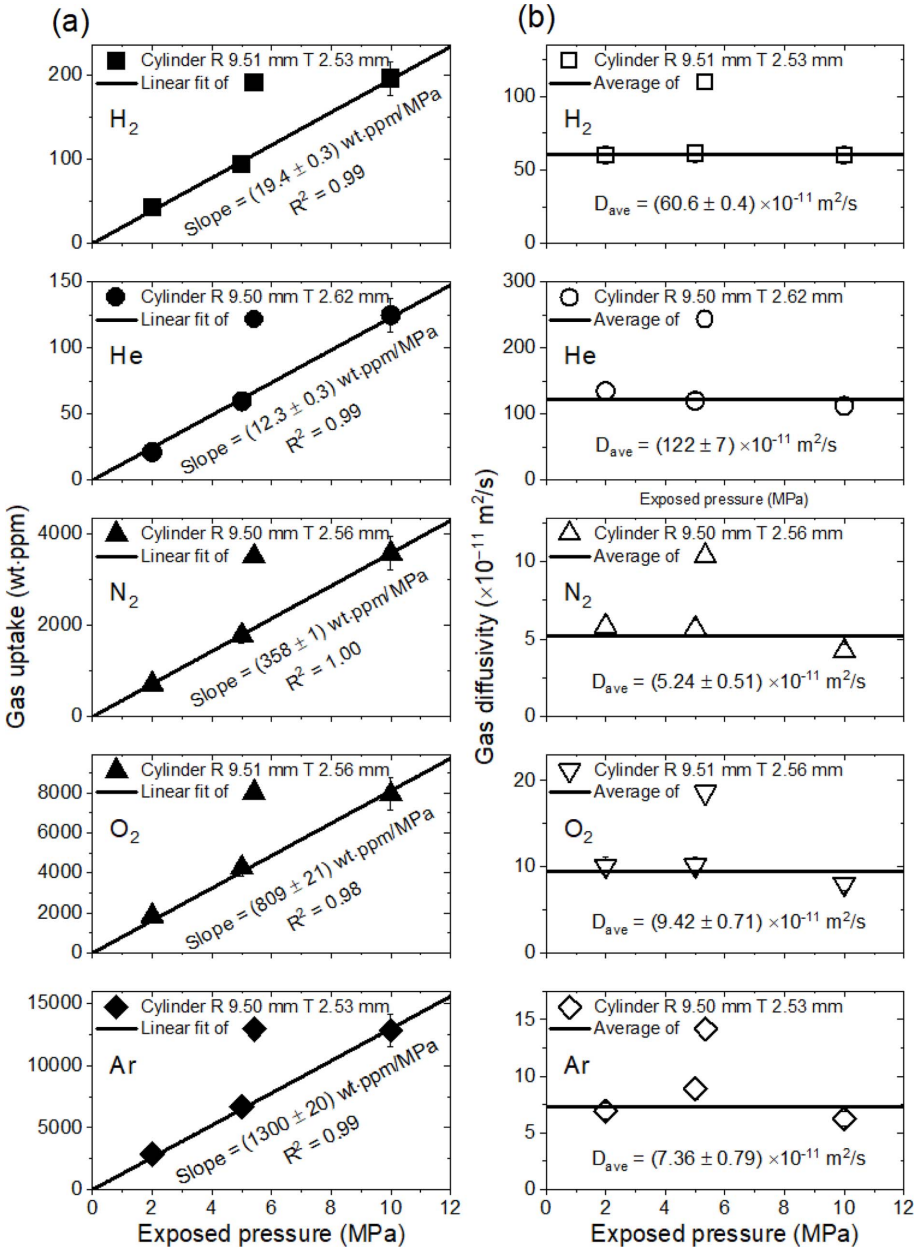

Fig. 5. (a) Gas uptake, (b) diffusivity versus exposed pressure for the five gases in a cylindrical-shaped EPDM. R and T represent the radius and thickness of cylindrical LDPE, respectively.

Table 1. Summary for solubility and diffusivity of five gases measured by VM in LDPE

Sensing method	Solubility [mol/m^3·MPa]					Diffusivity [× 10^{-11} m^2/s]				
	H_2	He	N_2	O_2	Ar	H_2	He	N_2	O_2	Ar
VM	5.78	1.81	7.70	15.00	18.89	24.2	54.3	1.93	3.35	2.54

Table 2. Summary for solubility and diffusivity of five gases measured by VM in EPDM

Sensing method	Solubility [mol/m^3·MPa]					Diffusivity [× 10^{-11} m^2/s]				
	H_2	He	N_2	O_2	Ar	H_2	He	N_2	O_2	Ar
VM	10.49	3.35	13.93	27.56	35.47	60.60	122.0	5.24	9.42	7.36

for five distinct gases. As shown in *Fig.* 4(a), the black line linearly fitted to the gas uptake data has squared correlation coefficients of $R^2 > 0.98$, indicating that LDPE absorbs the all gas molecules in their molecular state without undergoing dissociation or chemical reactions, following Henry's law. In *Fig.* 4(b), the diffusivity does not exhibit a substantial dependence on the exposed pressure. The black error bars in *Fig.* 4(a) and (b) represent the expanded measurement uncertainty of 10 %, as estimated in an earlier study. In *Fig.* 4(a), the slope of gas uptake for the exposed pressure is represented by a slope value. The diffusivity in *Fig.* 4(b) is represented by the average value (D_{ave}) of the three data points, as indicated by the black horizontal line.

Fig. 5 depict the gas uptake and diffusivity versus the exposed pressure for EPDM for five gases. The gas absorption behavior of EPDM in *Fig.* 5(a) satisfactorily follows Henry's law to a maximum of 10 MPa, as indicated by the black line, $R^2 > 0.98$. As displayed in *Fig.* 5(b), the diffusivity is not pressure dependent. Thus, the average diffusivity is taken, as indicated by the black horizontal line.

Moreover, gas solubility (S) is obtained from gas uptake versus pressure from *Figs.* 4 and 5 as follows:[149,156-158]

$$S\left[\frac{mol}{m^2 \cdot MPa}\right] = \frac{(C_\infty/\text{pressure})\left[\frac{wt \cdot ppm}{MPa}\right] \times 10^6 \times d\left[\frac{g}{m^2}\right]}{m_g\left[\frac{g}{mol}\right]} \quad (5)$$

m_g is molar mass of the enriched gas and d is density of the sample. The solubility and diffusivity in volumetric sensor determined for H_2, He, N_2, O_2 and Ar gases in LDPE and EPDM sample are shown in *Tables* 1 and 2, respectively. Clear differences in permeation parameters depending on the gas species were observed for both LDPE and EPDM samples. For all tested samples, gas solubility consistently decreased in the following order: $S_{Ar} > S_{O2} > S_{N2} > S_{H2} > S_{He}$. Although various factors contribute to gas permeation properties, solubility is known to have a linear relationship with the critical temperature of the gas [38, 42]. The critical temperatures of the gases are H_2: 33.0 K, He: 3.4 K, N_2: 126.2 K, O_2: 154.6 K, and Ar: 150.7 K. These data confirm that solubility tends to increase with higher critical temperatures.

In the analysis of diffusivity, emphasis was placed on the effective molecular size rather than the critical temperature. The diffusivity in LDPE and EPDM samples decreased in the order: $D_{He} > D_{H2} > D_{O2} > D_{Ar} > D_{N2}$. The effective molecular size of permeating gases significantly influences diffusivity, and the logarithm of diffusivity is known to correlate linearly with the kinetic diameter of gas molecules [38, 42]. The kinetic diameters of the gases are as follows: H_2: 0.289 nm, He: 0.260 nm, N_2: 0.364 nm, O_2: 0.346 nm, and Ar: 0.343 nm. These diameters represent the effective size of the interaction zone that can cause molecular scattering, directly relating to the mean free path of molecules in a gas. Therefore, diffusivity generally decreases as the kinetic diameter of the gas molecules increases.

In *Tables* 1 and 2, the solubility and diffusivity in two specimens for volumetric sensor have 10 % relative expanded uncertainty for measured value.

Table 3. Performance of volumetric image sensor

Performance	Volumetric measurement
Sensitivity	16.43 wt·ppm/mL
Resolution	0.08 wt·ppm
Stability	0.2 %
Measuring range	Max. 1400 wt·ppm
Response time	~1 s
FOM	0.4 %

The solubility and diffusivity results obtained from the volumetric method will be compared with those obtained from manometric method with corresponding estimated relative uncertainty.

3.2. Performance of volumetric image gas sensor

The performance of the volumetric gas sensing system using an image processing algorithm and a digital camera was evaluated. The performance test results, including sensitivity, resolution, stability, measuring range, response time and figure of merit (FOM), are shown in *Table* 3. Sensitivity in the VM sensor is defined as the change in mass concentration relative to the change in measured volume. The obtained sensitivity was 16.43 wt·ppm/mL. A sensor with higher sensitivity typically offers better resolution. The resolution of the VM sensor is determined by the minimum measurable volume of 0.005 mL, corresponding to a mass concentration of 0.08 wt·ppm. To further improve the resolution, the inner volume of the graduated cylinder can be reduced, or the number of specimens can be increased, which would enhance both sensitivity and resolution.

The stability of the volumetric sensor is quantified by the standard deviation of measurements taken over 24 hours after gas emission from the specimen is completed. This was determined to be below 0.2 % of the mass concentration for the VM sensor. The measuring range in VM sensor is obtained as the maximum allowable concentration per mass of specimen within graduated cylinder with inner volumes. The measuring range for VM was 1400 wt·ppm which can be adjusted by varying the sample mass and cylinder volume. The gas sensor's volume response is almost instantaneous, occurring within ~1 second of gas emission. FOM is defined as the standard deviation between measured data and theoretical value calculated using Eq. (4). FOM value below 0.4 % for VM sensor, indicates an excellent agreement between the theoretical and measured values. Additionally, the measurable range, resolution and sensitivity can be fine-tuned by adjusting the sample number and cylinder inner volume.

4. Conclusions

Gas sensors are crucial for ensuring safety and protecting property in gas-related facilities. We have developed gas sensing system that utilizes volumetric measurements with a graduated cylinder, coupled with an image processing algorithm and a digital camera. The variation in the water level, observed through pixel shifts in the graduated cylinder, is directly linked to changes in water volume caused by the released gas, allowing for precise measurement of gas concentration. By integrating a diffusion-permeation analysis program, this volumetric image-based gas sensor is capable of detecting not only gas concentrations but also solubility/diffusivity from gas-enriched specimens under high-pressure conditions.

The portable volumetric gas sensor systems showcased several key performance metrics: a low detection limit for gas content, a measurable range of up to 1400 wt·ppm, stability of 0.2 % and a rapid responsing time within 1 second. Additionally, the sensors' insensitivity to temperature and pressure fluctuations made them highly reliable for gas detection. The high-performance systems, utilizing volumetric measurements, successfully demonstrated real-time monitoring and characterization of pure gases such as H_2, He, N_2, O_2 and Ar. The sensors effectively measured gas uptake and diffusivity, considering influencing factors and calculating expanded uncertainty. The main features of developed gas sensing method are summarized as:

– **Cost-effective and simple techniques**: The volumetric method provides affordable and straightforward solutions for evaluating gas uptake

and diffusivity in gas charged polymers.

– **Stability against temperature and pressure variations**: The volumetric method is stable under fluctuations in temperature and pressure. The method is independent on a specimen sizes, shapes and gas types.
– **Adjustable sensitivity and range**: The volumetric method offers adjustable sensitivity, resolution, and measuring range, allowing for customization based on specific application requirements.
– **No chemical interaction**: The sensing method functions without any interaction between the gas molecules and the sensor, ensuring accurate mea- surements without altering the composition of the gas.
– **Visible gas release monitoring:** The volumetric method provides visual gas monitoring of gas release by changes in water level.

Although the proposed sensor exhibits limited selectivity for distinguishing specific gases, its rapid response and high sensitivity make it highly effective for initial monitoring in mixed-gas environments, particularly for rapid detection of gas leaks. Future studies will focus on optimizing the sensor structure to further improve its performance, expanding its potential for practical real-time gas leak detection applications.

Acknowledgements

This research was supported by the Development of Reliability Measurement Technology for Hydrogen Refueling Station funded by the Korea Research Institute of Standards and Science (KRISS - 2024 - GP2024-0010).

References

1. Z. Wang, L. Zhu, J. Zhang, J. Wang, X. Cui, X. Chen, W. Liu, H. Ma, J. Wang, and W. Yan, *Sens. Actuators B Chem.*, **418**, 136276 (2024). https://doi.org/10.1016/j.snb.2024.136276
2. B. C. Yadav and P. Kumar, In 'Compex and Composite Metal Oxides for Gas, VOC and Humidity Sensors', p133-157, Elsevier, 2024. https://doi.org/10.1016/C2021-0-02857-13
3. J. K. Jung, I. G. Kim, K. S. Chung, and U. B. Baek, Mater. Chem. Phys., **267**, 124653 (2021). https://doi.org/10.1016/j.matchemphys.2021.124653
4. J. K. Jung and J. H. Lee, *Sci. Rep.*, **14**(1), 1967 (2024). https://doi.org/10.1038/s41598-024-52168-3
5. J. Li, Y. Li, and W. Zeng, *Sens. Actuators A Phys.*, **365**, 114890 (2024). https://doi.org/10.1016/j.sna.2023.114890
6. Y. Yang, S. Zheng, X. Fu, and H. Zhang, *Optik*, **158**, 602-609 (2018). https://doi.org/10.1016/j.ijleo.2017.12.151
7. P. Mohapatra, S. Panigrahi, and J. Amamcharla, *J. Food Meas. Charact.*, **9**(2), 121-129 (2015). https://doi.org/10.1007/s11694-014-9200-9
8. J. K. Jung, I. G. Kim, and K. T. Kim, *Current Applied Physics*, **21**, 43-49 (2021). https://doi.org/10.1016/j.cap.2020.10.003
9. T. J. Johnson, R. L. Sams, and S. W. Sharpe, Proceedings of the Chemical and Biological Point Sensors for Homeland Defense, SPIE, Bellingham, WA, USA, 159-167 (2004). https://doi.org/10.1117/12.515604
10. H. Wessels and H. J. Keding, Sixth European Symposium on Space Environmental Control Systems, European Space Agency, Noordwijk, The Netherlands, 823-828 (1997).
11. J. K. Jung, I. G. Kim, K. T. Kim, U. B. Baek, and S. H. Nahm, *Current Applied Physics*, **26**, 9-15 (2021). https://doi.org/10.1016/j.cap.2021.03.005
12. S. E. Kayacık, A. H. Schrotenboer, E. Ursavas, and I. F. A. Vis, *Sustain. Energy Grids Netw.*, **38**, 101394 (2024). https://doi.org/10.1016/j.segan.2024.101394
13. I. Amez, B. Castells, D. León, and R. Paredes, *Fuel*, **381**, 133663 (2025). https://doi.org/10.1016/j.fuel.2024.133663
14. M. Wu, L. Bai, F. Deng, J. He, K. Song, and H. Li, *Coord. Chem. Rev.*, **523**, 216259 (2025). https://doi.org/10.1016/j.ccr.2024.216259
15. M. Tang, C. Qin, X. Sun, M. Li, Y. Wang, J. Cao, and Y. Wang, *Appl. Phys. A*, **130**(10), 741 (2024). https://doi.org/10.1007/s00339-024-07905-w
16. H. M. Kang, J. W. Bae, J. H. Lee, Y. M. Yun, S. K. Jeon, N. K. Chung, J. K. Jung, U. B. Baek, J. H. Lee, Y. W. Kim, and M. C. Choi, *Polymers*, **16**(8), 1065 (2024). https://doi.org/10.3390/polym16081065
17. A. Tom, D. K. Singh, V. K. Shaw, P. V. Abhijith, S.

Sajana, P. S. Kirandas, V. Dixit, V. Kamble, S. P. Pai, and D. Jaiswal-Nagar, *Rev. Sci. Instrum.*, **95**(8), 085003 (2024). https://doi.org/10.1063/5.0202940
18. R. Venkatesan, R. Harun, H. M. Yusoff, and M. A. Razak, *Process Saf. Prog.*, **43**(S1), S161-S169 (2024).
19. J. K. Jung, K. T. Kim, N. K. Chung, U. B. Baek, and S. H. Nahm, *Polymers*, **14**(7), 1468 (2022). https://doi.org/10.3390/polym14071468
20. J. N. Lu, Y. Huang, Y. S. Xia, L. Z. Dong, L. Zhang, J. J. Liu, L. G. Xie, J. Liu, and Y. Q. Lan, *Carbon Energy*, **6**(3), e396 (2024). https://doi.org/10.1002/cey2.396
21. P. Soundarrajan and F. Schweighardt, In 'Hydrogen fuel: Production, Transport, and Storage', pp. 495-534, R. B. Gupta, Ed., CRC Press, Boca Raton, 2008.
22. W. J. Buttner, M. B. Post, R. Burgess, and C. Rivkin, *Int. J. Hydrog. Energy*, **36**(3), 2462-2470 (2011). https://doi.org/10.1016/j.ijhydene.2010.04.176
23. Y. Wang, Y. Pang, H. Xu, A. Martinez, and K. S. Chen, *Energy Environ. Sci.*, **15**(6), 2288-2328 (2022). https://doi.org/10.1039/D2EE00790H
24. H. Fujiwara, H. Ono, K. Onoue, and S. Nishimura, *Int. J. Hydrog. Energy*, **45**(53), 29082-29094 (2020). https://doi.org/10.1016/j.ijhydene.2020.07.215
25. B. L. Choi, J. K. Jung, U. B. Baek, and B. H. Choi, *Polymers*, **14**(5), 861 (2022). https://doi.org/10.3390/polym14050861
26. E. R. Duranty, T. J. Roosendaal, S. G. Pitman, J. C. Tucker, S. L. Owsley, J. D. Suter, and K. J. Alvine, *Rev. Sci. Instrum.*, **88**(9), 095114 (2017). https://doi.org/10.1063/1.5001836
27. H. M. Kang, M. C. Choi, J. H. Lee, Y. M. Yun, J. S. Jang, N. K. Chung, S. K. Jeon, J. K. Jung, J. H. Lee, J. H. Lee, Y. W. Chang, and J. W. Bae, *Polymers*, **14**(6), 1151 (2022). https://doi.org/10.3390/polym14061151
28. I. Profatilova, F. Fouda-Onana, M. Heitzmann, T. Bacquart, A. Morris, J. Warren, F. Haloua, and P.-A. Jacques, *Int. J. Hydrog. Energy*, **65**, 837-843 (2024). https://doi.org/10.1016/j.ijhydene.2024.04.055
29. C. H. Lee, J. K. Jung, S. K. Jeon, K. S. Ryu, and U. B. Baek, *Journal of Magnetics*, **22**(3), 478-482 (2017). https://doi.org/10.4283/JMAG.2017.22.3.478
30. T. Iijima, T. Abe, and H. Itoga, *Synthesiology*, **8**(2), 62-69 (2015). https://doi.org/10.5571/syntheng.8.2_61
31. S. U. Zhanguo, W. Zhang, A. Abdulwahab, S. Saleem, Y. Yao, A. Deifalla, and M. Taghavi, *Process Saf. Environ. Prot.*, **173**, 317-331 (2023). https://doi.org/10.1016/j.psep.2023.03.015
32. J. K. Jung, J. H. Lee, S. K. Jeon, U. B. Baek, S. H. Lee, C. H. Lee, and W. J. Moon, *Polymers*, **15**(1), 162 (2023). https://doi.org/10.3390/polym15010162
33. J. K. Jung, U. B. Baek, S. H. Lee, M. C. Choi, and J. W. Bae, *J. Polym. Sci.*, **61**(6), 460-471 (2022). https://doi.org/10.1002/pol.20220494
34. S. Toghyani, E. Baniasadi, and E. Afshari, *Int. J. Hydrog. Energy*, **46**(47), 24271-24285 (2021). https://doi.org/10.1016/j.ijhydene.2021.05.026
35. Y.-H. Percival Zhang, J.-H. Xu, and J.-J. Zhong, *Int. J. Energy Res.*, **37**(7), 769-779 (2013). https://doi.org/10.1002/er.2897
36. B. Flamm, C. Peter, F. N. Büchi, and J. Lygeros, *Appl. Energy*, **281**, 116031 (2021). https://doi.org/10.1016/j.apenergy.2020.116031
37. W. Kuang, W. D. Bennett, T. J. Roosendaal, B. W. Arey, A. Dohnalkova, G. Petrossian, and K. L. Simmons, *Tribol. Int.*, **153**, 106627 (2021). https://doi.org/10.1016/j.triboint.2020.106627
38. J.-H. Lee, Y.-W. Kim, and J.-K. Jung, *Polymers*, **15**(19), 4019 (2023). https://doi.org/10.3390/polym15194019
39. J. H. Lee, Y. W. Kim, D. J. Kim, N. K. Chung, and J. K. Jung, *Polymers*, **16**(2), 280 (2024). https://doi.org/10.3390/polym16020280
40. J. H. Lee, Y. W. Kim, N. K. Chung, H. M. Kang, W. J. Moon, M. Chan Choi, and J. K. Jung, *Polymer*, **311**, 127552 (2024). https://doi.org/10.1016/j.polymer.2024.127552
41. C. H. Lee, J. K. Jung, K. S. Kim, and C. J. Kim, *Sci. Rep.*, **14**(1), 5319 (2024). https://doi.org/10.1038/s41598-024-55101-w
42. J. K. Jung, J. H. Lee, J. S. Jang, N. K. Chung, C. Y. Park, U. B. Baek, and S. H. Nahm, *Sci. Rep.*, **12**(1), 3328 (2022). https://doi.org/10.1038/s41598-022-07321-1
43. Y. Moon, H. Lee, J. Jung, and H. Han, *Sci. Rep.*, **13**(1), 7846 (2023). https://doi.org/10.1038/s41598-023-34565-2
44. G.-H. Kim, Y.-I. Moon, J.-K. Jung, M.-C. Choi, and J.-W. Bae, *Polymers*, **14**(1), 155 (2022). https://doi.org/10.3390/polym14010155
45. J. K. Jung, C. H. Lee, U. B. Baek, M. C. Choi, and J. W. Bae, *Polymers*, **14**(3), 592 (2022). https://doi.org/

10.3390/polym14030592
46. C. Liu, R. Zhang, L. Tian, C. Wang, X. Xu, Y. Pei, and L. Yuxing, *Nat. Gas Ind.*, **42**(9), 145-156 (2022).
47. D. B. Smith, B. J. Frame, L. M. Anovitz, and C. Makselon, Proceedings of the ASME 2016 Pressure Vessels and Piping Conference. Volume 6B: Materials and Fabrication, American Society of Mechanical Engineers, Vancouver, British Columbia, Canada, V06BT06A036 (2016). https://doi.org/10.1115/PVP2016-63683
48. Y.-S. Chou and J. W. Stevenson, *J. Power Sources*, **191**(2), 384-389 (2009). https://doi.org/10.1016/j.jpowsour.2009.02.052
49. G. Li, J. Zhang, J. Chai, Z. Ni, and Y. Yan, *Int. J. Hydrog. Energy*, **89**, 738-745 (2024). https://doi.org/10.1016/j.ijhydene.2024.09.361
50. S. Yuan, S. Zhang, J. Wei, Y. Gao, Y. Zhu, and H. Wang, *Int. J. Hydrog. Energy*, **91**, 555-573 (2024). https://doi.org/10.1016/j.ijhydene.2024.10.066
51. S. Tanaka, A. Higashitani, K. Sugie, and M. Esashi, *IEEJ Trans. Sens. Micromachines*, 123(9), 340-345 (2003). https://doi.org/10.1541/ieejsmas.123.340
52. J. LePree, *Chem. Eng.*, **116**(6), 19-22 (2009). https://doi.org/10.2174/138620709787581738
53. R. Checchetto, M. Scarpa, M. G. De Angelis, and M. Minelli, *J. Membr. Sci.*, **659**, 120768 (2022). https://doi.org/10.1016/j.memsci.2022.120768
54. S. K. Jeon, J. K. Jung, N. K. Chung, U. B. Baek, and S. H. Nahm, *Polymers*, **14**, 2233 (2022). https://doi.org/10.3390/polym14112233
55. D. Brown, S. Neyertz, M. J. T. Raaijmakers, and N. E. Benes, *J. Membr. Sci.*, **577**, 113-128 (2019). https://doi.org/10.1016/j.memsci.2019.01.039
56. G. Sun, C. Wang, J. Jia, H. Zhang, Y. Hu, Y. Liu, and D. Zhang, *J. Electron. Mater.*, **53**(7), 3426-3437 (2024). https://doi.org/10.1007/s11664-024-11146-1
57. J.-H. Lo, K. M. Smits, Y. Cho, G. P. Duggan, and S. N. Riddick, *Environ. Pollut.*, **341**, 122810 (2024). https://doi.org/10.1016/j.envpol.2023.122810
58. S. A. Sadovnikov, S. V. Yakovlev, N. S. Kravtsova, O. A. Romanovskii, and D. A. Tuzhilkin, *Sens. Int.*, **6**, 100307 (2025). https://doi.org/10.1016/j.sintl.2024.100307
59. J. Meng, S. Balendhran, Y. Sabri, S. K. Bhargava, and K. B. Crozier, *Microsyst. Nanoeng.*, **10**, 74 (2024). https://doi.org/10.1038/s41378-024-00697-2
60. H. Schlicke, R. Maletz, C. Dornack, and A. Fery, *Small*, **20**(48), 2403502 (2024). https://doi.org/10.1002/smll.202403502
61. J. F. D. S. Petruci, P. R. Fortes, V. Kokoric, A. Wilk, I. M. Raimundo, A. A. Cardoso, and B. Mizaikoff, *Analyst*, **139**(1), 198-203 (2014). https://doi.org/10.1039/C3AN01793A
62. A. Theodosiou, K. Kalli, and O. Sapir-Henderson, *IEEE Sens. J.*, **24**(13), 20669-20673 (2024). https://doi.org/10.1109/JSEN.2024.3400369
63. M. A. Z. Chowdhury and M. A. Oehlschlaeger, *Sensors*, **24**(6), 1873 (2024). https://doi.org/10.3390/s24061873
64. C. Mitmit, E. Goldenberg, and E. M. M. Tan, *Sens. Actuators A Phys.*, **351**, 114164 (2023). https://doi.org/10.1016/j.sna.2023.114164
65. X. L. Yu, F. Li, L. H. Chen, and X. Y. Chang, *Lasers Eng.*, **23**(1-2), 1-17 (2012).
66. G. Li, K. Ma, Y. Jiao, X. Zhang, Z. Zhang, Y. Wu, and Z. Yan, *Microw. Opt. Technol. Lett.*, **65**(5), 1047-1053 (2023). https://doi.org/10.1002/mop.33115
67. B. Molleman, E. Alessi, F. Passaniti, and K. Daly, *Inf. Process. Agric.*, **11**(4), 573-580 (2024). https://doi.org/10.1016/j.inpa.2023.11.001
68. S.-K. Kwon, J.-N. Kim, H.-G. Byun, and H.-J. Kim, *Electrochem. Commun.*, **169**, 107834 (2024). https://doi.org/10.1016/j.elecom.2024.107834
69. M. Eshkobilova, Z. Smanova, J. Begimqulov, S. Suvankulov, and E. Abdurakhmanov, *AIP Conf. Proc.*, 3244(1), 050007 (2024). https://doi.org/10.1063/5.0242048
70. M. T. N. Nguyen and J. S. Lee, *Chemosensors*, **12**(11), 233 (2024). https://doi.org/10.3390/chemosensors12110233
71. A. Alaghmandfard, S. Fardindoost, A. L. Frencken, and M. Hoorfar, *Ceram. Int.*, **50**(17), 29026-29043 (2024). https://doi.org/10.1016/j.ceramint.2024.05.259
72. Y. Li, Z. Yuan, H. Ji, F. Meng, and H. Wang, *IEEE Trans. Ind. Electron.*, **71**(9), 11661-11670 (2024). https://doi.org/10.1109/TIE.2023.3329254
73. Z. Liao, Z. Yuan, H. Gao, and F. Meng, *Sens. Actuators B Chem.*, **412**, 135825 (2024). https://doi.org/10.1016/j.snb.2024.135825
74. L. Gao, Y. Tian, A. Hussain, Y. Guan, and G. Xu, *Anal. Bioanal. Chem.*, **416**(16), 3697-3715 (2024). https://doi.org/10.1007/s00216-024-05213-z

75. G. Korotcenkov, *Sensors*, **24**(12), 3861 (2024). https://doi.org/10.3390/s24123861
76. H. Ji, H. Zhu, R. Zhang, Z. Yuan, and F. Meng, *Sens. Actuators B Chem.*, **408**, 135553 (2024). https://doi.org/10.1016/j.snb.2024.135553
77. T. Sahoo and P. Kale, *Adv. Mater. Interfaces*, **8**(23), 2100649 (2021). https://doi.org/10.1002/admi.202100649
78. C. Schultealbert, J. Amann, T. Baur, and A. Schütze, *Atmosphere*, **12**(3), 366 (2021). https://doi.org/10.3390/atmos12030366
79. X. Zhang, B. Ojha, H. Bichlmaier, I. Hartmann, and H. Kohler, *Sensors*, **23**(10), 4679 (2023). https://doi.org/10.3390/s23104679
80. W. Bowen, *Heliyon*, **9**(3), e14055 (2023).
81. S. Tamura and N. Imanaka, *Bunseki Kagaku*, **70**(6), 327-334 (2021). https://doi.org/10.2116/bunsekikagaku.70.327
82. P. Rodlamul, S. Tamura, and N. Imanaka, *Bull. Chem. Soc. Jpn.*, **92**(3), 585-591 (2019). https://doi.org/10.1246/bcsj.20180284
83. W. Jang, J.-S. Park, K.-W. Lee, and Y. Roh, *Micro Nano Syst. Lett.*, **6**(1), 7 (2018). https://doi.org/10.1186/s40486-018-0069-y
84. H. Oigawa, M. Shimojima, T. Tsuno, and T. Ueda, *Sens. Mater.*, **30**(5), 1103-1114 (2018). https://doi.org/10.18494/SAM.2018.1906
85. H. Hadano, A. Miyagi, T. Okuno, Y. Nagawa, and Y. Ishiguro, *ECS Trans.*, **75**(16), 195-198 (2016). https://doi.org/10.1149/07516.0195ecsta
86. R. Xie, S. Guan, and Z. Tan, *Opt. Commun.*, **574**, 131105 (2025). https://doi.org/10.1016/j.optcom.2024.131105
87. Y. Zhang, M. Wang, P. Yu, and Z. Liu, *Sensors*, **22**(20), 7949 (2022). https://doi.org/10.3390/s22207949
88. Y. I. Moon, J. K. Jung, G. H. Kim, and K. S. Chung, *Phys. B Condens. Matter.*, **608**, 412870 (2021). https://doi.org/10.1016/j.physb.2021.412870
89. J. Cao, K. Zhang, R. Yang, and Z. Wang, Proceedings of the 8th World Congress on Intelligent Control and Automation, IEEE, Jinan, China, 7021-7025 (2010). https://doi.org/10.1109/WCICA.2010.5554250
90. M. Gruber, M. Bohling, H. Knuppertz, M. Mogl, and H. Winkelmann, Latin America Optics and Photonics Conference, OSA, MB32 (2010). https://doi.org/10.1364/LAOP.2010.MB32
91. A. van Brakel, E. Austin, C. Grivas, M. N. Petrovich, and D. J. Richardson, Proceedings of SPIE - The International Society for Optical Engineering, SPIE, 70046A (2008). https://doi.org/10.1117/12.786114
92. A. Yarai and T. Nakanishi, *Rev. Sci. Instrum.*, **75**(10), 3237-3241 (2004). https://doi.org/10.1063/1.1791338
93. J. P. Dakin, H. O. Edwards, and B. H. Weigl, *Sens. Actuators B Chem.*, **29**(1-3), 87-93 (1995). https://doi.org/10.1016/0925-4005(95)01667-8
94. J. K. Jung, Y. I. Moon, K. S. Chung, and K. T. Kim, *MACROMOLECULAR RESEARCH*, **28**, 596-604 (2020). https://doi.org/10.1007/s13233-020-8080-6
95. Y. Miao, *Beijing Gongye Daxue Xuebao/J. Beijing Univ. Technol.*, **48**(3), 312-330 (2022).
96. Z. Weiss, J. Čapek, Z. Kačenka, O. Ekrt, J. Kopeček, M. Losertová, and D. Vojtěch, *J. Anal. At. Spectrom.*, 39(4), 996-1003 (2024). https://doi.org/10.1039/D3JA00434A
97. D. Bizyaev, *Mon. Not. R. Astron. Soc. Lett.*, **528**(1), L146-L151 (2024). https://doi.org/10.1093/mnrasl/slad186
98. M. Mazzaglia, L. Celona, S. Gammino, E. Naselli, R. Reitano, G. Torrisi, and D. Mascali, *Nuovo Cimento Soc. Ital. Fis. Sez. C*, **44**(2-3), 58 (2021). https://doi.org/10.1393/ncc/i2021-21058-9
99. C. Lee, N. Leconte, J. Kim, D. Cho, I.-W. Lyo, and E. J. Choi, *Carbon*, **103**, 109-114 (2016). https://doi.org/10.1016/j.carbon.2016.03.008
100. J. R. Saffell and N. A. Martin, *J. Test. Eval.*, **52**(5), 2675-2684 (2024). https://doi.org/10.1520/JTE20230675
101. W. M. Seleka, K. E. Ramohlola, K. D. Modibane, and E. Makhado, *Int. J. Hydrog. Energy*, **68**, 940-954 (2024). https://doi.org/10.1016/j.ijhydene.2024.04.240
102. S. R. Mishra, V. Gadore, and M. Ahmaruzzaman, *Mater. Lett.*, **359**, 135946 (2024). https://doi.org/10.1016/j.matlet.2024.135946
103. T. Cowen, S. Grammatikos, and M. Cheffena, *Analyst*, **149**(8), 2428-2435 (2024). https://doi.org/10.1039/D4AN00045E
104. A. Asilian and S. M. Zanjani, *Majlesi J. Electr. Eng.*, **18**(1), 21-32 (2024). https://doi.org/10.30486/mjee.2023.1988651.1157
105. W. Chen, D. Liao, and S. Wu, *J. Electrochem. Soc.*, **171**(11), 117519 (2024). https://doi.org/10.1149/1945-7111/ad8f67
106. S. I. Kaya, L. Karadurmus, M. Yence, M. G. Caglayan, and S. A. Ozkan, In 'Recent Trends and Perspectives on

Electrochemical Sensors for Environmental Monitoring', pp551-575, S. A. Ozkan, Ed., Elsevier, Cambridge, 2024. https://doi.org/10.1016/B978-0-443-13388-6.00017-6
107. R. Lakhmi, J.-P. Viricelle, R. Alrammouz, and M. Rieu, *Sensors*, **24**(2), 658 (2024). https://doi.org/10.3390/s24020658
108. Y. Ha, J. Kwon, S. Choi, and D. Jung, *J. Sens. Sci. Technol.*, **32**(5), 290-294 (2023). https://doi.org/10.46670/JSST.2023.32.5.290
109. Y. Wang, Y. Pan, Y. Jiang, M. Xu, and J. Jiang, *Microchem. J.*, **190**, 108715 (2023). https://doi.org/10.1016/j.microc.2023.108715
110. A. K. Farquhar, G. S. Henshaw, and D. E. Williams, *Sens. Actuators A Phys.*, **354**, 114254 (2023). https://doi.org/10.1016/j.sna.2023.114254
111. N. Ma, S. Halley, K. Ramaiyan, F. Garzon, and L.-k. Tsui, *ECS Sens. Plus*, **2**(1), 011402 (2023). https://doi.org/10.2139/ssrn.4328217
112. A. S. Kalyakin and A. N. Volkov, *Chim. Techno Acta*, **10**(1), 202310109 (2023). https://doi.org/10.1016/j.jtice.2024.105940
113. T. Adrikowski, *Prz. Elektrotech.*, **99**(3), 79-85 (2023). http://dx.doi.org/10.15199/48.2023.03.12
114. T. Puttasakul, C. Tancharoen, W. Sukjee, and C. Sangma, *IEEE Sens. J.*, **22**(23), 22368-22373 (2022). https://doi.org/10.1109/JSEN.2022.3214067
115. Y. Triana, G. Ogata, and Y. Einaga, *Curr. Opin. Electrochem.*, **36**, 101113 (2022). https://doi.org/10.1016/j.coelec.2022.101113
116. S.-J. Kweon, J.-H. Park, C.-O. Park, H.-J. Yoo, and S. Ha, *Sensors*, **22**(11), 3965 (2022). https://doi.org/10.3390/s22113965
117. A. S. Kalyakin, D. A. Medvedev, and A. N. Volkov, *J. Electrochem. Soc.*, **169**(5), 057530 (2022). https://doi.org/10.1149/1945-7111/ac725d
118. A. K. Farquhar, G. S. Henshaw, and D. E. Williams, *ACS Sensors*, **6**(3), 1295-1304 (2021). https://doi.org/10.1021/acssensors.0c02589
119. J. K. Jung, I. G. Kim, K. S. Chung, Y.-I. Kim, and D. H. Kim, *Sci. Rep.*, **11**(1), 17092 (2021). https://doi.org/10.1038/s41598-021-96266-y
120. J. K. Jung, I. G. Kim, K. S. Chung, and U. B. Baek, *Sci. Rep.*, **11**(1), 4859 (2021). https://doi.org/10.1038/s41598-021-83692-1
121. J. K. Jung, K.-T. Kim, and K. S. Chung, *Mater. Chem. Phys.*, **276**, 125364 (2022). https://doi.org/10.1016/j.matchemphys.2021.125364
122. J. K. Jung, I. G. Kim, K. T. Kim, K. S. Ryu, and K. S. Chung, *Polym. Test.*, **93**, 107016 (2021). https://doi.org/10.1016/j.polymertesting.2020.107016
123. R. Slater, K. Tharmaratnam, S. Belnour, M. K.-H. Auth, R. Muhammed, C. Spray, D. Wang, B. de Lacy Costello, M. García-Fiñana, S. Allen, and C. Probert, *Sensors*, **24**(15), 5079 (2024). https://doi.org/10.3390/s24155079
124. K.-W. Lou, C.-L. Ho, and Y.-P. Ho, 2023 IEEE 16th International Conference on Nano/Molecular Medicine & Engineering (NANOMED), IEEE, Okinawa, Japan, 194-198 (2023). https://doi.org/10.1109/NANOMED59780.2023.10404347
125. M. Koehne, E. Djaw, M. Schoellner, T. Sauerwald, and G. Zeh, 2024 IEEE International Instrumentation and Measurement Technology Conference (I2MTC), IEEE, Glasgow, United Kingdom, 1-6 (2024). https://doi.org/10.1109/I2MTC60896.2024.10561210
126. F. Hardoyono and K. Windhani, *Flavour Fragr. J.*, **38**(6), 451-463 (2023). https://doi.org/10.1002/ffj.3759
127. Z. Huang, W. Yang, Y. Zhang, J. Yin, X. Sun, J. Sun, G. Ren, S. Tian, P. Wang, and H. Wan, *Anal. Chem.*, **96**(45), 17960-17968 (2024). https://doi.org/10.1021/acs.analchem.4c02561
128. A. Hinojo, E. Lujan, J. Abella, and S. Colominas, *Fusion Eng. Des.*, **204**, 114483 (2024). https://doi.org/10.1016/j.fusengdes.2024.114483
129. J. Hu, H. Qu, W. Pang, and X. Duan, *Sensors*, **21**(20), 6800 (2021). https://doi.org/10.3390/s21206800
130. A. H. Alinoori and S. Masoum, *Anal. Chem.*, **90**(11), 6635-6642 (2018). https://doi.org/10.1021/acs.analchem.8b00426
131. S. Y. Oh, *Phytochem. Anal.*, **29**(3), 275-283 (2018). https://doi.org/10.1002/pca.2740
132. D. Yadav, A. Shrivastava, A. Sircar, P. Dhorajiya, A. Muniya, and R. P. Bhattacharyay, *Fusion Eng. Des.*, **200**, 114189 (2024). https://doi.org/10.1016/j.fusengdes.2024.114189
133. H.-C. Lau, J.-B. Yu, H.-W. Lee, J.-S. Huh, and J.-O. Lim, *Sensors*, **17**(8), 1783 (2017). https://doi.org/10.3390/s17081783
134. C. Wang, J. Yang, J. Li, C. Luo, X. Xu, and F. Qian,

Int. J. Hydrog. Energy, **48**(80), 31377-31391 (2023). https://doi.org/10.1016/j.ijhydene.2023.04.167

135. J. K. Jung, I. G. Kim, S. K. Jeon, and K. S. Chung, *Rubber Chem. Technol.*, **94**(4), 688-703 (2021). https://doi.org/10.5254/rct.21.79880
136. X. Zhu, W. Ahmed, K. Schmidt, R. Barroso, S. J. Fowler, and C. F. Blanford, *IEEE Trans. Instrum. Meas.*, **73**(99), 1-8 (2024). https://doi.org/10.1109/TIM.2024.3485428
137. L. Quercia, I. Khomenko, R. Capuano, M. Tonezzer, R. Paolesse, E. Martinelli, A. Catini, F. Biasioli, and C. Di Natale, *Sens. Actuators B Chem.*, **347**, 130580 (2021). https://doi.org/10.1016/j.snb.2021.130580
138. Y. R. Shaltaeva, B. I. Podlepetsky, and V. S. Pershenkov, *Eur. J. Mass Spectrom.*, **23**(4), 217-224 (2017). https://doi.org/10.1177/1469066717720795
139. J. A. Imonigie, R. N. Walters, and M. M. Gribb, *Instrum. Sci. Technol.*, **34**(6), 677-695 (2006). https://doi.org/10.1080/10739140600964010
140. C. Pérès, F. Begnaud, and J.-L. Berdagué, *Anal. Chem.*, **74**(10), 2279-2283 (2002). https://doi.org/10.1021/ac0111558
141. P. Li, S. Li, W. Zhao, A. Zhang, J. Liu, Y. Wang, X. Zhang, and J. Liu, *J. Future Foods*, **5**(1), 50-56 (2025). https://doi.org/10.1016/j.jfutfo.2024.01.004
142. P. D. Zander, F. Rubach, and A. Martínez-García, *Rapid Commun. Mass Spectrom.*, **39**(3), e9943 (2025). https://doi.org/10.1002/rcm.9943
143. X. He and H. H. Jeleń, *Food Chem.*, **465**, 142004 (2025). https://doi.org/10.1016/j.foodchem.2024.142004
144. G. Feng, J. Li, J. Liu, and R. Tan, *Food Chem.*, **465**, 142012 (2025). https://doi.org/10.1016/j.foodchem.2024.142012
145. B. Quintanilla-Casas, B. Torres-Cobos, R. Bro, F. Guardiola, S. Vichi, and A. Tres, *Curr. Opin. Food Sci.*, **61**, 101235 (2025). https://doi.org/10.1016/j.cofs.2024. 101235
146. J. Hao, F. Xu, D. Yang, B. Wang, Y. Qiao, and Y. Tian, *Renew. Sustain. Energy Rev.*, **208**, 115090 (2025). https://doi.org/10.1016/j.rser.2024.115090
147. M. Vinaixa, A. Vergara, C. Duran, E. Llobet, C. Badia, J. Brezmes, X. Vilanova, and X. Correig, *Sens. Actuators B Chem.*, **106**(1), 67-75 (2005). https://doi.org/10.1016/j.snb.2004.05.038
148. J. H. Lee and J. K. Jung, *Sensors*, **24**(23), 7699 (2024). https://doi.org/10.3390/s24237699
149. J. K. Jung, I. G. Kim, S. K. Jeon, K.-T. Kim, U. B. Baek, and S. H. Nahm, *Polym. Test.*, **99**, 107147 (2021). https://doi.org/10.1016/j.polymertesting.2021.107147
150. J. K. Jung, J. H. Lee, S. K. Jeon, N. H. Tak, N. K. Chung, U. B. Baek, S. H. Lee, C. H. Lee, M. C. Choi, H. M. Kang, J. W. Bae, and W. J. Moon, *Int. J. Mol. Sci.*, **24**(3), 2865 (2023). https://doi.org/10.3390/ijms24032865
151. J. K. Jung, K.-T. Kim, and U. B. Baek, *Curr. Appl. Phys.*, **37**, 19-26 (2022). https://doi.org/10.1016/j.cap.2022.02.005
152. J. K. Jung, *Polymers*, **16**(5), 723 (2024). https://doi.org/10.3390/polym16050723
153. J. Crank, 'The Mathematics of Diffusion', Clarendon Press, Oxford, 1979.
154. A. Demarez, A. G. Hock, and F. A. Meunier, *Acta Metall.*, **2**(2), 214-223 (1954). https://doi.org/10.1016/0001-6160(54)90162-5
155. J. A. Nelder and R. Mead, *Comput. J.*, **7**(4), 308-313 (1965). https://doi.org/10.1093/comjnl/7.4.308
156. J. K. Jung, J. H. Lee, Y. W. Kim, and N. K. Chung, *Sens. Actuators B Chem.*, **418**, 136240 (2024). https://doi.org/10.1016/j.snb.2024.136240
157. J. K. Jung, C. H. Lee, M. S. Son, J. H. Lee, U. B. Baek, K. S. Chung, M. C. Choi, and J. W. Bae, *Polymers*, **14**(4), 700 (2022). https://doi.org/10.3390/polym14040700
158. J. K. Jung, K. T. Kim, U. B. Baek, and S. H. Nahm, *Polymers*, **14**(4), 756 (2022). https://doi.org/10.3390/polym14040756